"©2010 IEEE. Personal use of this material is permitted. However, permission to reprint/republish this material for advertising or promotional purposes or for creating new collective works for resale or redistribution to servers or lists, or to reuse any copyrighted component of this work in other works must be obtained from the IEEE."

Performance Analysis of TDMA Relay Protocols Over Nakagami-m Fading

Saman Atapattu, *Student Member, IEEE*, Nandana Rajatheva, *Senior Member, IEEE*, and Chintha Tellambura, *Senior Member, IEEE*

***Abstract*—Several time-division multiple-access (TDMA) cooperative wireless relay protocols and their performances have recently been developed by Nabar, Bolcskei, and Kneubuhler. Their work, however, is limited to an upper bound-based performance analysis for Rayleigh fading. We thus provide an exact analysis of two of their protocols in single-relay and multiple-relay networks over independent identically distributed (i.i.d.) Nakagami-m fading channels. Our analysis is focused on an Alamouti-coded system with two-stage protocols, fixed-gain amplify-and-forward (AF) relays, and maximal ratio combiner (MRC) reception. The performance metrics are the capacity, the diversity order, and the symbol error rate (SER). The closed-form moment-generating function (MGF) of the total end-to-end signal-to-noise ratio (SNR) is derived. The MGF is then used to derive the diversity order and the SER of M-ary phase-shift keying (M-PSK) and M-ary quadrature amplitude modulation (M-QAM). It is found that the end-to-end SNR for relaying with orthogonal channels is higher than that of nonorthogonal relay channels. The diversity order of a multiple-relay network (n relays) in a Nakagami-m environment is shown to be $(n+1)m$. The closed-form SER expressions for relay–destination links with high SNRs and static relay–destination links are derived. Numerical and simulation results are provided to verify the analysis.**

***Index Terms*—Amplify and forward (AF), diversity, Nakagami-m fading, relays, space–time coding (STC).**

I. Introduction

THE IDEA of using intermediate nodes (relays) to help the signal transmission between the source and the destination has received significant attention in the wireless community. Such cooperative relying helps mitigate deep fading in wireless networks by creating a virtual distributed multiple-input–multiple-output (MIMO) system [1]–[3]. Because of the benefits of cooperative relaying techniques, several standardization groups, such as IEEE 802.16 and IEEE 802.11, have incorporated relaying into their emerging standards. For instance, the Mobile Multihop Relaying Group has already defined the multihop relay system in the baseline IEEE 802.16j [4].

The common relay types are decode-and-forward (DF) relays and amplify-and-forward (AF) relays. A DF relay demodulates and decodes the received signal from the source before retransmission, whereas an AF relay simply amplifies and retransmits the noisy version of the received signal. The AF relays can be fixed gain (the knowledge of the received average power is required) or variable gain (the knowledge of instantaneous channel gain is required) [3], [5]. Not only does the AF mode place a smaller processing load than the DF mode but can also outperform the latter (e.g., when there is a poor source to relay link) [6].

Relays can be used with conventional multiple access methods [7]–[9], such as time-division multiple access (TDMA), frequency-division multiple access (FDMA), and code-division multiple access (CDMA). Three different TDMA-based cooperative protocols (Protocols I, II, and III) have been introduced in [10]. These protocols implement varying degrees of broadcasting and receiver collision in the network. Protocol I realizes broadcasting with receive collision, Protocol II realizes broadcasting with no receive collision, and Protocol III does not implement broadcasting but realizes receive collision. Wireless relay networks using distributed space–time coding (DSTC) can utilize these protocols. Space–time coding (STC) typically uses two-stage cooperative protocols, where in the first stage the source transmits to relays. In the second stage, the relays use a distributed code and retransmit to the destination.

In this paper, we focus on a detailed performance analysis of these protocols. It is important to asses their theoretical performance limits given their degrees of broadcasting and receive collision in the network. Our analysis provides a better understanding of their performance limits in Nakagami-m fading channels. Since these protocols use DSTC, our results can also help in better DSTC design. Furthermore, our results may also be used for optimal power allocation among network nodes. Different DSTC designs can be found in the literature. The authors in [11] analyze the mutual information and outage probability of a relay network that utilizes a suitable STC in the second stage to simultaneously transmit the signals on the subchannels. However, this model requires the decoding of the received signal. In [12], the authors introduce a "distributed" linear dispersion code where the relays need not decode the received signal.

Since closed-form expressions for capacity and symbol error rate (SER) and/or bit error rate (BER) of relay networks are difficult, numerical methods or approximations are developed in the literature. For instance [13], a lower bound, which is not tight at medium and high signal-to-noise ratios (SNRs), for the BER of a collaborative dual-hop multiple-relay wireless network is derived for Nakagami-m fading. The asymptotic

Manuscript received March 4, 2009; revised June 13, 2009. First published August 18, 2009; current version published January 20, 2010. The review of this paper was coordinated by Prof. H.-H. Chen.

S. Atapattu and C. Tellambura are with the Department of Electrical and Computer Engineering, University of Alberta, Edmonton, AB T6G 2V4, Canada (e-mail: atapattu@ece.ualberta.ca; chintha@ece.ualberta.ca).

N. Rajatheva is with the Telecommunications Field of Study, School of Engineering and Technology, Asian Institute of Technology, Pathumthani 12120, Thailand (e-mail: rajath@ait.ac.th).

Digital Object Identifier 10.1109/TVT.2009.2029980

0018-9545/$26.00 © 2009 IEEE

Authorized licensed use limited to: UNIVERSITY OF ALBERTA. Downloaded on January 20, 2010 at 12:24 from IEEE Xplore. Restrictions apply.

SER for general cooperative links (an arbitrary number of cooperative branches and hops) is analyzed for Rayleigh fading in [14]. A tighter lower bound on the average error performance is derived in [15] for the same network as in [13]. The asymptotic outage behavior is investigated in terms of coding gain and diversity order for AF relaying [16]. Reference [17] analyzes the performance of relay selection over Rayleigh fading. Furthermore, multihop relaying in different fading channels is analyzed in [18] and [19]. Our previous work analyzed TDMA-based relay protocols in terms of the exact SER [20]–[22].

The Nakagami-m distribution is widely employed for characterizing wireless channel fading. Since it sometimes models empirical data better than Rayleigh, log-normal, or Rician distributions, performance analysis for this model may prove useful for a wider class of wireless channels [23]. That is why we analyze the TDMA relay protocols over Nakagami-m fading. In [24], protocols similar to [10] have been analyzed in terms of the diversity–multiplexing tradeoff, although the results are limited to Rayleigh fading. The authors of [24] establish an upper bound on the achievable diversity–multiplexing tradeoff for single and multiple relays. Since the performance of TDMA relay Protocols I and III of [10] over Nakagami-m fading is not available, this paper analyzes their performance. To the best of our knowledge, exact performance analysis of these two protocols has not previously been available in the literature.

The main contributions of this paper are as follows: The performance of Protocols I and II and the Alamouti scheme with a maximal ratio combining (MRC) receiver at the destination are considered. The main cases are the following: Case 1—single relay and nonorthogonal transmission in time slots 2 and 4; Case 2—single relay and orthogonal transmission in time slots 2 and 4; and Case 3—multiple relay and orthogonal transmission. Fixed-gain AF relays are considered. Since an exact closed-form expression for the moment-generating function (MGF) of end-to-end SNR can be used to derive the performance [15], [25], [26], the closed-form MGF for these cases is derived. The MGF is used to derive the SER of M-ary phase-shift keying (M-PSK) and M-ary quadrature amplitude modulation (M-QAM) and the diversity order. The end-to-end SNR of relaying with orthogonal channels is higher than that of nonorthogonal channels. The diversity order of a multiple-relay network (n relays) in a Nakagami-m environment is shown to be $(n+1)m$. Numerical and simulation results are provided to verify the analysis.

This paper is organized as follows: Section II describes the system model and the two TDMA relay protocols. Input–output relations and signal-to-noise (SNR) expressions are derived in Section III. In Section IV, the closed-form expressions for the MGF of end-to-end SNRs are presented. In Section V, the performance of two protocols with M-PSK and M-QAM is analyzed in terms of the capacity, the SER, and the diversity order. The numerical and simulation results are presented in Section VI. The concluding remarks are made in Section VII. The detailed steps of the derivation of the MGF are presented in the Appendix.

Notation: $\mathbb{E}(\cdot)$, $\mathbb{V}ar(\cdot)$, $\Gamma(\cdot)$, and $|\mathbf{a}|$ denote the expectation operator, the variance, the Gamma function, and the magnitude of the complex value $\mathbf{a}$, respectively. The superscripts ^{T}, ^{H}, and * stand for the transpose, the conjugate transpose, and the element-wise conjugate, respectively. $X \rightarrow Y$ signifies the link between nodes X and Y.

TABLE I
TRANSMISSION PROTOCOLS

Time Slot / Protocol	I	II
1, 3	$S \rightarrow D, R$	$S \rightarrow R$
2, 4	$S \rightarrow D$, $R \rightarrow D$	$S \rightarrow D$, $R \rightarrow D$

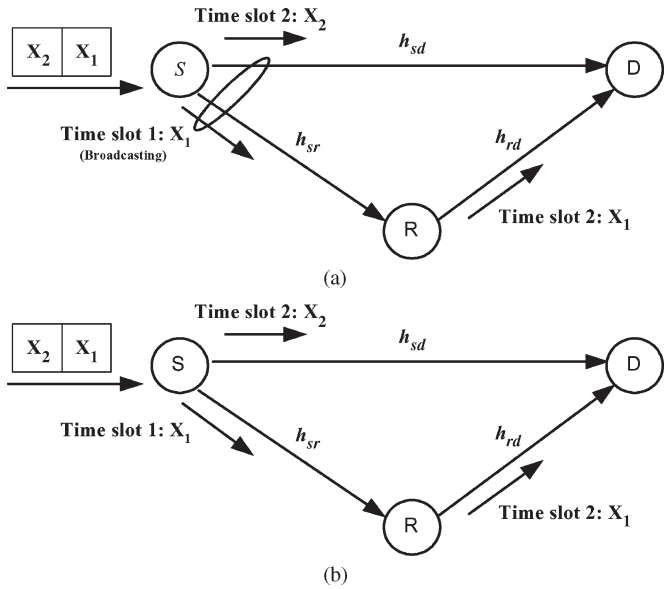

Fig. 1. (a) Protocol I and (b) Protocol II for a single-relay wireless network with the source S, the destination D, and the relay R.

II. SYSTEM MODEL

This section describes the two TDMA-based protocols of [10]: 1) the signal model and 2) the fading channel. A wireless network with a single-user relay channel having one source, single relay, and one destination is considered.

A. Protocols

The two different protocols for the transmission of STC in a distributed manner [10] are considered. The Alamouti code [27] $\mathbf{C} = \begin{bmatrix} x_1 & x_2 \\ -x_2^* & x_1^* \end{bmatrix}$ is transmitted over two-stage protocols, as summarized in Table I.[1] In Protocol I, source S broadcasts x_1 for both relay R and destination D, whereas in Protocol II, x_1 is received by relay R only in the first time slot. In the second time slot, in both protocols, relay R forwards an amplified version of the first received signal, and source S transmits x_2 (see Fig. 1).[2] Similarly, source S serially transmits $-x_2^*$ and x_1^* in the third and fourth time slots, respectively, over the

[1]The two protocols, i.e., Protocols I and II, appear in [10] as Protocols I and III, respectively.

[2]Fig. 1 illustrates the transmission of x_1 and x_2 in the first and second time slots, respectively.

Authorized licensed use limited to: UNIVERSITY OF ALBERTA. Downloaded on January 20, 2010 at 12:24 from IEEE Xplore. Restrictions apply.

direct and relay-assisted channels. In Protocol III, source only communicates with relay in the first and third time slots. A similar communication as Protocol I takes place in the second and forth time slots. The main advantage is that the transmitter does not require multiple antennas to create a MIMO system with this particular (distributed) space–time transmission. Every transmitter is equipped with a single antenna. Since a particular symbol x_i ($i = 1$ and 2) is transmitted through both direct and relayed paths within the flat fading interval, diversity can be extracted.

B. Channel Model

The relay system is assumed to operate over independent identically distributed (i.i.d.) Nakagami-m fading channels. Perfect synchronization and perfect channel state information are available (i.e., the $S \to R$ channel is known to the relay, whereas the $S \to D$, $R \to D$, and $S \to R$ channels are known to the destination D). The fading coefficient for the $X \to Y$ link is h_{xy}, and the magnitude of h_{xy} is Nakagami-m distributed with the probability density function (pdf) given by [28]

$$f_{|h_{xy}|}(t) = \frac{2m^m t^{2m-1}}{\Gamma(m)} \exp(-mt^2), \qquad t \geq 0 \tag{1}$$

where $\mathbb{E}(|h_{xy}|^2) = 1$. Then, $\alpha_{xy} = |h_{xy}|^2$ follows the gamma distribution pdf given by [29]

$$f_{\alpha_{xy}}(t) = \frac{m^m t^{m-1}}{\Gamma(m)} \exp(-mt), \qquad t \geq 0. \tag{2}$$

Additive white Gaussian noise (AWGN) samples are circularly symmetric complex Gaussian random variables with mean zero and variance N_0 [i.e., $n \sim \mathcal{CN}(0, N_0)$].

III. Input–Output Relation and Signal-to-Noise Ratio

The input–output relation for the Alamouti code transmission can be derived as an equivalent single-input–single-output (SISO) model. Thus, the end-to-end SNR is easily obtained. The following three different cases are analyzed for each protocol:

- *Case 1:* single-relay network with nonorthogonal channels;
- *Case 2:* single-relay network with orthogonal channels;
- *Case 3:* multiple-relay network.

In an orthogonal channel, the destination D receives two independent signals from source S and relay R either in the same time slot with two different frequency bands (FDMA) or in the same frequency band within two different time slots (TDMA). Otherwise, the transmission channel is nonorthogonal. The orthogonal channel assumption has already been used in [14] and [15]. Such orthogonal channels can also be realized by using CDMA technology.

A. Protocol I

Case 1: Here, destination D receives the superposition of the direct path signal and the relay-assisted path signal. The system model for a single-relay network is as follows: In the first time slot, the received signal at destination D may be written as

$$y_1 = \sqrt{E_{sd}} h_{sd} x_1 + n_1 \tag{3}$$

where $n_1 \sim \mathcal{CN}(0, N_0)$ denotes the AWGN term at destination D. Throughout this paper, E_{xy} is the average transmit signal energy from node X to node Y. The time slot index is 1, which is the subscript of y, x, and n. Without loss of generality, the signal constellation power is normalized to unity (i.e., $\mathbb{E}(|x_i^2|) = 1$).

In the first time slot, the received signal at relay R can be modeled as

$$y_r = \sqrt{E_{sr}} h_{sr} x_1 + n_r \tag{4}$$

where n_r is the AWGN sample at relay R. The relay normalizes the received signal by a factor of $\sqrt{\mathbb{E}(|y_r|^2)}$ to ensure unit average energy. Since the relay is AF fixed gain, the relay has the knowledge of the received average power. Further, normalization does not effect the overall SNR of the relay path. The normalized signal is $y_r/\sqrt{\mathbb{E}(|y_r|^2)} = y_r/\sqrt{E_{sr} + N_0}$. In the second time slot, destination D receives the combined signal from relay R and source S. The total effective noise at destination D $\tilde{n} = \sqrt{E_{rd}/(E_{sr} + N_0)} h_{rd} n_r + \tilde{n}_2$ can be model as $\tilde{n} \,|\, h_{rd} \sim \mathcal{CN}(0, N_0')$, where $N_0' = [(E_{rd}/(E_{sr} + N_0))|h_{rd}|^2 + 1]N_0$, $\omega^2 = (E_{rd}/(E_{sr} + N_0))|h_{rd}|^2 + 1$, and $\tilde{n}_2$ is the AWGN sample for the signal component received through the direct path. Finally, destination D normalizes the received signal by ω. The signal received at destination D can then be expressed as

$$y_2 = \frac{1}{\omega} \sqrt{\frac{E_{rd} E_{sr}}{E_{sr} + N_0}} h_{sr} h_{rd} x_1 + \frac{1}{\omega} \sqrt{E_{sd}} h_{sd} x_2 + n_2 \tag{5}$$

where $n_2 \,|\, h_{rd} \sim \mathcal{CN}(0, N_0)$. Similarly, the received signals at destination D for the third and fourth time slots can, respectively, be written as

$$y_3 = \sqrt{E_{sd}} h_{sd} (-x_2^*) + n_3 \tag{6}$$

$$y_4 = \frac{1}{\omega} \sqrt{\frac{E_{rd} E_{sr}}{E_{sr} + N_0}} h_{sr} h_{rd} (-x_2^*) + \frac{1}{\omega} \sqrt{E_{sd}} h_{sd} (x_1^*) + n_4. \tag{7}$$

By using (3) and (5)–(7), the input–output relationship for the Alamouti-coded Protocol I for Case 1 can be written as

$$\mathbf{Y} = \mathbf{H}\mathbf{X} + \mathbf{N} \tag{8}$$

where

$$\mathbf{Y}^T = [\, y_1 \quad y_2 \quad y_3^* \quad y_4^* \,]_{1\times 4}$$

$$\mathbf{N}^T = [\, n_1 \quad n_2 \quad n_3^* \quad n_4^* \,]_{1\times 4}$$

$$\mathbf{H}^{\mathbf{T}} = \begin{bmatrix} A & B & 0 & C^* \\ 0 & C & -A^* & -B^* \end{bmatrix}_{2\times 4}$$

$$\mathbf{X}^T = [\, x_1 \quad x_2 \,]_{1\times 2}$$

Authorized licensed use limited to: UNIVERSITY OF ALBERTA. Downloaded on January 20, 2010 at 12:24 from IEEE Xplore. Restrictions apply.

with $A = \sqrt{E_{sd}}h_{sd}$, $B = (1/\omega)\sqrt{E_{rd}E_{sr}/(E_{sr}+N_0)}h_{rd}h_{sr}$, and $C = \sqrt{E_{sd}}h_{sd}/\omega$.

MRC reception is performed at destination D. Thus, premultiplication of the received signal vector (8) by $\mathbf{H}^H$ yields the equivalent SISO model as

$$\begin{bmatrix} Y_1 \\ Y_2 \end{bmatrix} = \left[|A|^2 + |B|^2 + |C|^2\right] \begin{bmatrix} x_1 \\ x_2 \end{bmatrix} + \begin{bmatrix} N_1 \\ N_2 \end{bmatrix} \tag{9}$$

where $\mathbb{E}(N_i) = 0$, and $\mathbb{V}ar(N_i) = [|A|^2 + |B|^2 + |C|^2]N_0$ for $i = 1, 2$. Therefore, the total end-to-end SNR can be written as

$$\gamma = \frac{\left[|A|^2 + |B|^2 + |C|^2\right]}{N_0}. \tag{10}$$

Case 2: We consider the same protocol by assuming orthogonal $S \to D$ and $R \to D$ channels. The received signal at destination D in the first time slot in this case is the same as in (3), and it can be written as

$$y_{d1} = \sqrt{E_{sd}}h_{sd}x_1 + n_{d1} \tag{11}$$

where $n_{d1} \sim \mathcal{CN}(0, N_0)$ denotes the AWGN at destination D,[3] whereas destination D receives two independent signals through the relay path and the direct path within the second time slot. Clearly, the two signals have different noise variances (noise power) because of the noise contribution at relay R. Therefore, MRC requires noise normalization across the different diversity branches. Therefore, the receiver at destination D normalizes the relayed signal by ω. Finally, the signal received at destination D through the relay path and the direct path within the second time slot can, respectively, be expressed as

$$y_{r2} = \frac{1}{\omega}\sqrt{\frac{E_{sr}E_{rd}}{E_{rd}+N_0}}h_{sr}h_{rd}x_1 + n_{r2} \tag{12}$$

where $n_{r2} \,|\, h_{rd} \sim \mathcal{CN}(0, N_0)$, and

$$y_{d2} = \sqrt{E_{sd}}h_{sd}x_2 + n_{d2}. \tag{13}$$

Similarly, the received signal after the third and fourth time slots at the destination D receiver can be written as (11)–(13) for the two signal points $-x_2^*$ and x_1^*. Therefore, the input–output relationship for the Alamouti system with Protocol 1 under Case 2 can be written as $\mathbf{Y} = \mathbf{HX} + \mathbf{N}$, where

$$\mathbf{Y}^T = \begin{bmatrix} y_{d1} & y_{r2} & y_{d2} & y_{d3}^* & y_{r4}^* & y_{d4}^* \end{bmatrix}_{1\times 6}$$

$$\mathbf{H}^T = \begin{bmatrix} A & B & 0 & 0 & 0 & A^* \\ 0 & 0 & A & -A^* & -B^* & 0 \end{bmatrix}_{2\times 6}$$

$$\mathbf{N}^T = \begin{bmatrix} n_{d1} & n_{r2} & n_{d2} & n_{d3}^* & n_{r4}^* & n_{d4}^* \end{bmatrix}_{1\times 6}.$$

After MRC at destination D, the total end-to-end SNR can be written as

$$\gamma = \frac{\left[2|A|^2 + |B|^2\right]}{N_0}. \tag{14}$$

[3]In Cases 2 and 3, the first subscript of y and n denotes the path of the received signal (e.g., r and d denote the relay path and the direct path, respectively), and the second subscript denotes the time slot.

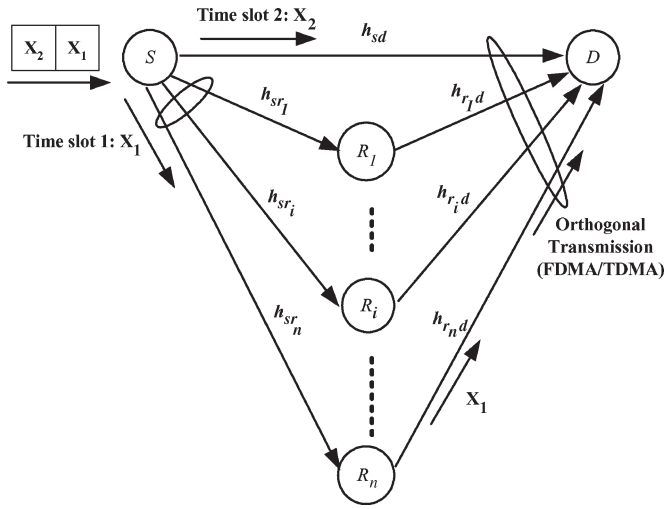

Fig. 2. Multiple-relay wireless network with n-number of relays R_i, $i = 1, 2, \ldots, n$, for Protocol I.

Case 3: In [22], the authors only analyzed multiple-relay network for Protocol II. In this section, the multiple-relay cooperative network is generalized to both protocols with n relays (see Fig. 2). Therefore, there are n number of cooperative links and one direct link between source S and destination D. We assume mutually orthogonal $S \to D$ and $R_i \to D$, $\forall i = 1, 2, \ldots, n$, channels. The received signals through these orthogonal channels can be MRC processed at destination D.

Similarly, in Case 2, the MRC at destination D should be preceded by noise normalization. The signals received at destination D through the direct path are the same as those in the previous case within the first and third time slots. After noise normalization, the received signal through the ith relay (R_i) in the second time slot can be written as

$$y_{r_i 2} = \frac{1}{\omega_i}\sqrt{\frac{E_{sr}E_{rd}}{E_{rd}+N_0}}h_{sr_i}h_{r_i d}x_1 + n_{r_i 2} \tag{15}$$

where ω_i is the noise normalization factor for the corresponding ith relay path. Since source S broadcasts the same signal to all relays, the same power (E_{sr}) should be transmitted toward $S \to R_i$. Although the transmitted power from the different relays can differ, we use the same (E_{rd}) for the sake of convenience.

After MRC reception at destination D, the effective end-to-end SNR can be expressed as

$$\gamma = \frac{\left[2|A|^2 + \sum_{i=1}^{n}|B_i|^2\right]}{N_0} \tag{16}$$

where $B_i = (1/\omega_i)\sqrt{E_{r_i d}E_{sr_i}/(E_{sr_i}+N_0)}h_{r_i d}h_{sr_i}$.

B. Protocol II

Protocol II is derived from Protocol I, since destination D only receives signals in the second and fourth time slots, as in (5) and (7), respectively. Therefore, the input–output relations for each case can easily be derived from the above formulation in Section III-A. As a result, we briefly review Case 1 only.

Authorized licensed use limited to: UNIVERSITY OF ALBERTA. Downloaded on January 20, 2010 at 12:24 from IEEE Xplore. Restrictions apply.

The corresponding matrices for (8) are $\mathbf{Y}^T = [y_2 \quad y_4^*]_{1\times 2}$, $\mathbf{H^T} = \begin{bmatrix} B & C^* \\ C & -B^* \end{bmatrix}_{2\times 2}$, and $\mathbf{N}^T = [n_2 \quad n_4^*]_{1\times 2}$. With MRC at destination D, (8) can be expressed in the form of the equivalent SISO form as in (9). Therefore, the total end-to-end SNR for Case 1 can be expressed as

$$\gamma = \frac{\left[|B|^2 + |C|^2\right]}{N_0}. \tag{17}$$

Similarly, the end-to-end SNRs for Cases 2 and 3 may, respectively, be written as

$$\gamma = \frac{\left[|A|^2 + |B|^2\right]}{N_0} \tag{18}$$

$$\gamma = \frac{\left[|A|^2 + \sum_{i=1}^{n} |B_i|^2\right]}{N_0}. \tag{19}$$

In Protocol I, all the links in all time are effectively utilized for a particular cooperative communication, whereas Protocol II does not. In the cooperative (ad hoc) scenario, destination D in Protocol II might be engaged in data/information exchange to another terminal during the first time slot, and this particular communication only takes place in source S to relay R link.

IV. Moment-Generating Function

Because closed-form expressions for the pdf of SNR for multiple-relay networks are not always available, the MGF approach can be used as an alternative and popular method of calculating the performance of digital systems over fading channels [30]. The SER expressions of common modulation formats can readily be incorporated with this approach [30]. We thus derive the closed-form MGF for each case.

A. Protocol I

Case 1: The total equivalent SNR in (10) can further be expressed as

$$\gamma = \left[E_{sd}|h_{sd}|^2 + \frac{E_{sd}|h_{sd}|^2}{\left[\frac{E_{rd}}{(E_{sr}+N_0)}|h_{rd}|^2 + 1\right]} + \frac{E_{sr}E_{rd}}{(E_{sr}+N_0)} \frac{|h_{sr}|^2|h_{rd}|^2}{\left[\frac{E_{rd}}{(E_{sr}+N_0)}|h_{rd}|^2 + 1\right]} \right] \frac{1}{N_0} \tag{20}$$

which is a function of all the fading coefficients h_{sd}, h_{sr}, and h_{rd}. For notational convenience, define the *unfaded* SNR of the link $A \to B$ as $\rho_{ab} = E_{ab}/N_0$ and the *power gain* of the link $A \to B$ as $|h_{ab}|^2 = \alpha_{ab}$. Therefore, all of the unfaded SNRs and power gains are $\rho_{sd} = E_{sd}/N_0$, $\rho_{sr} = E_{sr}/N_0$, $\rho_{rd} = E_{rd}/N_0$, and $|h_{sd}|^2 = \alpha_{sd}$, $|h_{sr}|^2 = \alpha_{sr}$, $|h_{rd}|^2 = \alpha_{rd}$. The MGF of γ can be written as

$$M_\gamma(t) = \mathbb{E}_{\alpha_{sd},\alpha_{sr},\alpha_{rd}}(e^{-t\gamma}) \tag{21}$$

where the expectation in (21) is to carried over α_{sd}, α_{sr}, and α_{rd}. The fading effects of all the links are modeled by mutually independent Nakagami-m random variables. See the Appendix for details. Therefore, the MGF of the end-to-end SNR can be expressed as

$$M_\gamma(t) = \frac{1}{\left[\left(1+\frac{\rho_{sr}}{m}t\right)\left(1+\frac{\rho_{sd}}{m}t\right)\right]^m} \times \left[1 + \sum_{u=1}^{2}\sum_{v=1}^{m} m^m A_{uv}(t)\left[\lambda_u(t)\right]^{m-v} \times \psi\left(m, m-v+1, m\lambda_u(t)\right)\right] \tag{22}$$

where $\psi(\alpha;\beta;z)$ is the confluent hypergeometric function of the second kind [31, eq. (9.211.4)], and $A_{uv}(t)$ and $\lambda_u(t)$ are also defined in the Appendix. Note that $\psi(\alpha;\beta;z)$ is a standard built-in function in common mathematical software packages such as Mathematica.

Cases 2 and 3: The $S \to D$ and $R_i \to D$ transmissions use orthogonal channels. Case 3 is considered below. As mentioned before, the power allocation for each relay can be fixed at E_{sr}. Although the transmitted power $(E_{r_i d})$ from different relays can differ, we use the same power E_{rd} for the sake of brevity of analysis (optimization of power allocation is an interesting topic but is not pursued here). The fading coefficients of the links $S \to R_i$ and $R_i \to D$ are h_{sr_i} and $h_{r_i d}$ for $i = 1, 2, \ldots, n$, respectively. Therefore, the normalization factor for the signal through the ith relay path is ω_i, where $\omega_i^2 = [E_{rd}/(E_{sr}+N_0)]|h_{r_i d}|^2 + 1$. The total equivalent SNR can be written as

$$\gamma = \left[2E_{sd}|h_{sd}|^2 + \sum_{i=1}^{n} \frac{1}{\omega_i^2} \frac{E_{sr}E_{rd}|h_{sr_i}|^2|h_{r_i d}|^2}{(E_{sr}+N_0)}\right] \frac{1}{N_0}. \tag{23}$$

Since all the channel coefficients are mutually independent and Nakagami-m distributed, similar to the previous case, after averaging over all the channel gains, the MGF of γ can be derived as

$$M_\gamma(t) = \frac{1}{\left[\left(1+\frac{2\rho_{sd}}{m}t\right)\left(1+\frac{\rho_{sr}}{m}t\right)^n\right]^m} \times \left[1 + \sum_{v=1}^{m} A_v(t) m^m \left[\mu(t)\right]^{m-v} \times \psi\left(m, m+1-v, m\mu(t)\right)\right]^n. \tag{24}$$

The MGF derivations $A_v(t)$ and $\mu(t)$ are given in the Appendix.

B. Protocol II

In Protocol I, the direct link $S \to D$ is utilized for communication in the first and third time slots, whereas in Protocol II, the direct link is not utilized. Therefore, destination D only receives one signal for each time slot, i.e., the second and fourth in Case 1. In the general case, with orthogonal transmission (see Case 3), destination D receives $(n+1)$ independent signals in the second and fourth time slots. According to the SNRs

Authorized licensed use limited to: UNIVERSITY OF ALBERTA. Downloaded on January 20, 2010 at 12:24 from IEEE Xplore. Restrictions apply.

given in (17)–(19), the MGF for Cases 1–3 can be evaluated as follows.

Case 1:

$$M_\gamma(t) = \frac{1}{\left[1+\frac{\rho_{sr}}{m}t\right]^m} \times \left[1+\sum_{u=1}^{2}\sum_{v=1}^{m} m^m A_{uv}(t)\left[\lambda_u(t)\right]^{m-v} \times \psi\left(m, m-v+1, m\lambda_u(t)\right)\right] \quad (25)$$

where

$$\lambda_1(t) = \frac{\frac{\rho_{sr}+1}{\rho_{rd}}}{1+\frac{\rho_{sr}}{m}t} \quad \lambda_2(t) = \frac{1+\frac{\rho_{sd}}{m}t}{\frac{\rho_{rd}}{\rho_{sr}+1}}.$$

Case 2:

$$M_\gamma(t) = \frac{1}{\left[\left(1+\frac{\rho_{sd}}{m}t\right)\left(1+\frac{\rho_{sr}}{m}t\right)\right]^m} \times \left[1+\sum_{v=1}^{m} A_v(t) m^m \left[\mu(t)\right]^{m-v} \times \psi\left(m, m+1-v, m\mu(t)\right)\right]. \quad (26)$$

Case 3:

$$M_\gamma(t) = \frac{1}{\left[\left(1+\frac{\rho_{sd}}{m}t\right)\left(1+\frac{\rho_{sr}}{m}t\right)^n\right]^m} \times \left[1+\sum_{v=1}^{m} A_v(t) m^m \left[\mu(t)\right]^{m-v} \times \psi\left(m, m+1-v, m\mu(t)\right)\right]^n. \quad (27)$$

V. Performance Analysis

This section describes the error analysis in terms of SER and capacity comparison of both protocols. Furthermore, the achievable diversity order is derived for the static $R_i \to D$ links.

A. Capacity

The use of the Alamouti code with MRC at destination D transforms the MIMO system into an equivalent SISO model for Protocols I and II (see Section III). When the effective SNR at the receiver is γ, the capacity is given by

$$\mathcal{C}(\gamma) = \log_2(1+\gamma) \text{ bits/s/Hz}. \quad (28)$$

In a conventional MIMO, the Alamouti code $\mathbf{C}$ is transmitted over two time slots from two colocated antennas. However, using these protocols, the Alamouti transmission requires at least four time slots in the case of single-relay nonorthogonal transmission. Since end-to-end SNRs for each case are evaluated in Section III, first, we compare the capacity of Protocol I ($C_{\rm I}$) and Protocol II ($C_{\rm II}$) by defining the *capacity ratio* as $C_R = C_{\rm I}/C_{\rm II}$. In both orthogonal and nonorthogonal cases, the bandwidth required is the same for both protocols. Therefore, C_R can be written as

$$C_R = \frac{\log_2(1+\gamma_{\rm Protocol\,I})}{\log_2(1+\gamma_{\rm Protocol\,II})}. \quad (29)$$

The system capacity totally depends on the effective SNRs at destination D. Since the normalization factor $\omega > 1$, we can write $\gamma_{\rm Protocol\,I} > \gamma_{\rm Protocol\,II}$ from (10) and (14). Therefore, Protocol I has a higher capacity than Protocol II. Simulation results are plotted in Fig. 3 between capacity ratio versus transmit SNR.

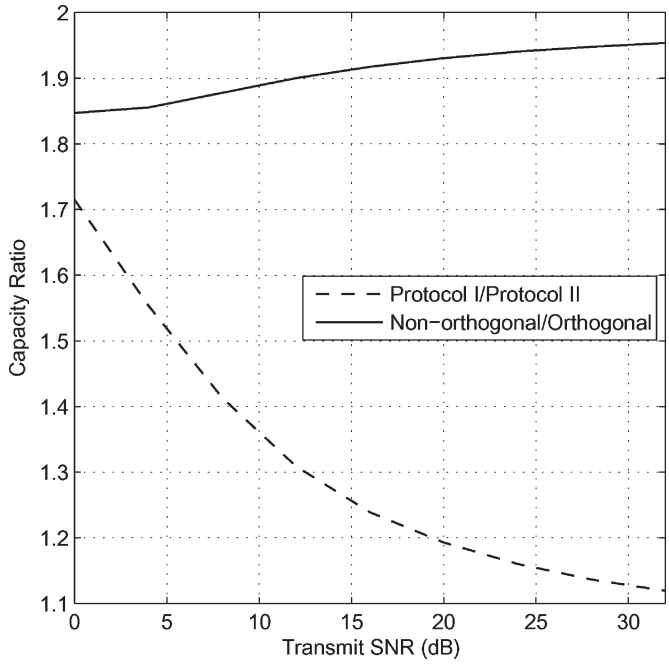

Fig. 3. Capacity ratio as a function of the transmit SNR over Nakagami-2 fading.

Protocol I yields a much better capacity in low SNRs, and both protocols have almost the same capacity at high SNR. The capacity ratio starts from 1.72 at 0 dB and asymptotically tends to unity as transmit SNR increases. In Protocol I, the direct link $S \to D$ is utilized for communication within the first and third time slots, whereas in Protocol II, the direct link is in free mode or engaging another communication.

Next, we compare the capacity of nonorthogonal and orthogonal transmission for a single relay. The transmission rate of the orthogonal case is half of that of the nonorthogonal case. Simulated values for the capacity ratio between these two cases are plotted in Fig. 3. The capacity ratio is around 1.847 for 0 dB, and it reaches to 2 for higher SNRs. Therefore, the capacity performance totally depends on the transmission rate at higher SNRs.

B. Diversity Order

The reduction in error rate due to the receiver processing multiple versions of the transmitted signal is quantified by *diversity order* or *diversity gain*. The diversity order is the

Authorized licensed use limited to: UNIVERSITY OF ALBERTA. Downloaded on January 20, 2010 at 12:24 from IEEE Xplore. Restrictions apply.

magnitude of the slope of the error probability versus SNR curve (log–log scale). This downward slope is measured in the high SNR region. The average error probability $\bar{p_e}$ may then be approximated as $\bar{p_e} \approx \tilde{c}\rho^{-g}$, where $\tilde{c}$ relates to the coding gain, ρ is the SNR, and g is the diversity order [32]. The diversity order can be found by using the Taylor series expansion of the pdf of the SNR near origin or by using the asymptotic value of the corresponding MGF near infinity [29], [32].

Here, we analyze two protocols in terms of diversity order. Our closed-form expression for the MGF of the end-to-end SNR in Section IV [see (24)] can be used to derive the diversity order. The $S \to D$, $S \to R_i$, and $R_i \to D$ channels are Nakagami-m fading.

According to [32, Prop. 3], if the MGF $M_\gamma(t)$ can be written in the form

$$|M_\gamma(t)| = b|t|^{-d} + o\left(|t|^{-d}\right) \tag{30}$$

as $t \to \infty$, then the diversity order of the system is given by d. We write (24) as

$$M_\gamma(t) = M_1(t)M_2(t) \tag{31}$$

where

$$M_1(t) = \frac{1}{\left[\left(1+\frac{2\rho_{sd}}{m}t\right)\left(1+\frac{\rho_{sr}}{m}t\right)^n\right]^m}$$

$$M_2(t) = \left[1 + \sum_{v=1}^{m} A_v(t) m^m \left[\mu(t)\right]^{m-v} \times \psi\left(m, m+1-v, m\mu(t)\right)\right]^n.$$

First, we consider that all the channels under Nakagami-m fading have $m > 1$. As $t \to \infty$, $\mu(t) \to 0$, the asymptotic formula of the second-order hypergeometric function is given by [33]

$$\psi(m, m+1-v, m\mu(t)) \approx \frac{\Gamma(m-v)}{\Gamma(m)}(m\mu(t))^{-(m-v)} \tag{32}$$

where $\Gamma(x)$ is the standard Gamma function. Further, $A_v(t)$ is in the form of $c_0 + c_1\mu(t) + c_2\mu(t)^2 + \cdots + c_{v-1}\mu(t)^{v-1}$, where $c_0, c_1, c_2, \ldots, c_{v-1}$ are real constants. Therefore, as $t \to \infty$, $A_v(t) \to$ constant, leads $M_2(t) \to C$, where C is a constant. Therefore, as $t \to \infty$, (24) can be expressed as

$$M_\gamma(t) \approx \frac{C}{\left[\frac{2\rho_{sd}}{m}\left(\frac{\rho_{sr}}{m}\right)^n\right]^m t^{m(n+1)}}. \tag{33}$$

By using (30) and (31), the asymptotic MGF in (33) shows that a cooperative network with n relays over a Nakagami-m fading environment archives the diversity order $d = (n+1)m$. The parameter m is the fading figure or shape factor that indicates the severity of fading. Since multipath scattering with different clusters of reflected waves acts as diversity branches, this achievable diversity order makes sense. For example, a diversity order of 1 is achieved for a single-relay network, and a diversity order of $(n+1)$ is achieved for an n-relay network in Rayleigh fading $(m = 1)$.

C. SER

The derived MGF can be used to evaluate the SER of each protocol under M-PSK and M-QAM.

1) M-PSK: The average SER for M-PSK can be written as [29]

$$P_e = \frac{1}{\pi}\int_0^{(M-1)\pi/M} M_\gamma\left(\frac{g_{\text{psk}}}{\sin^2\theta}\right) d\theta \tag{34}$$

where $g_{\text{psk}} = \sin^2(\pi/M)$.

2) M-QAM: Square M-QAM signals that have constellation size $M = 2^k$ with an even k are considered. The average SER over the generalized fading channels is given [29] as

$$P_e = \frac{4}{\pi}\left(1 - \frac{1}{\sqrt{M}}\right)\int_0^{\pi/2} M_\gamma\left(\frac{g_{\text{qam}}}{\sin^2\theta}\right) d\theta - \frac{4}{\pi}\left(1 - \frac{1}{\sqrt{M}}\right)^2 \int_0^{\pi/4} M_\gamma\left(\frac{g_{\text{qam}}}{\sin^2\theta}\right) d\theta \tag{35}$$

where $g_{\text{qam}} = 3/2(M-1)$.

Closed-form solutions for the exact SER in the general case seem analytically intractable. However, efficient numerical algorithms are readily available for (34) and (35). We use Mathematica, which provides adaptive algorithms that recursively subdivide the integration region. The precision level can readily be controlled. The availability of such tools ensure that the MGF and (34) and (35) combined with numerical algorithms provide an efficient and accurate solution. The numerical results and simulation results are discussed in Section VI.

3) Closed-Form SER Expressions: A closed-form SER can be derived for $R_i \to D$ links with high SNRs and static $R_i \to D$ links. The static $R_i \to D$ link means that the channels $R_i \to D$ are AWGN (i.e., $h_{r_i d} = 1$) [10] and that the other links are effected by Nakagami-m fading. Physically, this scenario corresponds to one where line-of-sight $R_i \to D$ channels. The corresponding MGFs of the two cases can be approximated as

$$M_\gamma(t) = \frac{1}{\left[1+\gamma_1(m,\rho_{sd})t\right]^m\left[1+\gamma_2(m,\rho_{sr},\rho_{rd})t\right]^{nm}} \tag{36}$$

where $\gamma_1(m,\rho_{sd}) = 2\rho_{sd}/m$ and $\gamma_2(m,\rho_{sr},\rho_{rd}) = \rho_{sr}/m$ for $R_i \to D$ links with high SNRs, and $\gamma_2(m,\rho_{sr},\rho_{rd}) = \rho_{sr}\rho_{rd}/m(\rho_{sr}+\rho_{rd}+1)$ for static $R_i \to D$ links.

From [29, eq. (5A.58)], the SER expression for (34) with the MGF in (36) can be evaluated in closed form as given in (37), shown at the bottom of the next page.

Similarly, in the case of any M-PSK and any M-QAM modulation schemes, closed-form SER expressions can be found for the Rayleigh fading channels $(m = 1)$ based on [29, eq. (5A.56)].

Authorized licensed use limited to: UNIVERSITY OF ALBERTA. Downloaded on January 20, 2010 at 12:24 from IEEE Xplore. Restrictions apply.

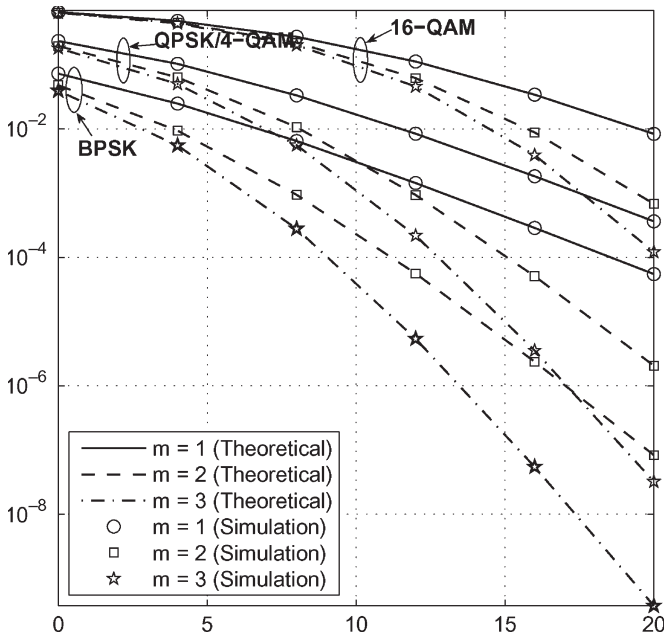

Fig. 4. Simulated and theoretical SER as a function of transmit SNR in Protocol I for M-PSK and M-QAM.

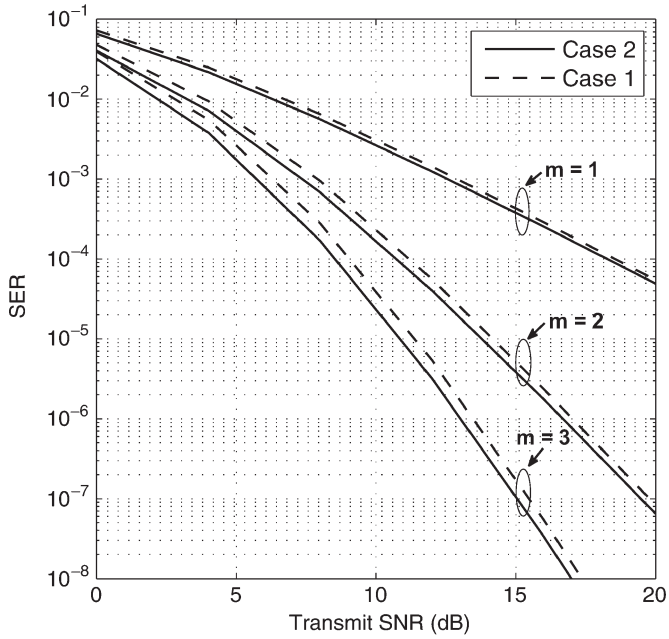

Fig. 5. SER variation of Cases 1 and 2 as a function of the transmit SNR in Protocol I for BPSK.

VI. Numerical and Simulation Results

This section provides simulation and analytical results for Protocols I and II. The performance metrics are the capacity, the diversity order, and the SER. Alamouti-coded symbols are randomly generated for binary phase shift keying (BPSK), quaternary phase shift keying (QPSK), and 16-quadrature amplitude modulation (16-QAM). The AWGN samples are complex Gaussian variables with mean zero and variance N_0. Three Nakagami variables (h_{sd}, h_{sr}, h_{rd}) are independently generated. About 10^{10} and 10^{15} number of symbols are used for simulations. The performance curves are plotted in terms of average SER (or capacity ratio) versus the transmit SNR (ρ dB) of $S \to D$, $S \to R_i$, and $R_i \to D$ links. We assume that $S \to D$, $S \to R_i$, and $R_i \to D$ links have the same transmit SNR.

Fig. 4 shows the SER performance of Protocol I for BPSK, QPSK, 4-QAM, and 16-QAM with $m = 1$ (Rayleigh fading), $m = 2$, and $m = 3$. For the numerical results, the integral formulas (34) and (35) are used for M-PSK and M-QAM, respectively. Clearly, the analytical results perfectly match with their simulation counterparts, confirming the accuracy of the analysis. As m increases, curves show higher diversity order as our analytical result. Since the diversity order only depends on parameter m and number of relays n, the SER curves for a particular m value are almost parallel in medium and high SNRs, irrespective of their modulation format.

Fig. 5 shows the comparison of the error performance between Cases 1 and 2 for the BPSK modulation scheme under Protocol I. As $A > C$ in (10) and (14), Case 2 has better end-to-end SNR, leading to a significant improvement in the SER performance over Case 1. In the former, destination D receives independent signals through the orthogonal channels, whereas in the latter, destination D receives a superposition signal. At high SNR approximation in (37), $\gamma_1(m, \rho_{sd})$ is ρ_{sd}/m and

$$P_e = \frac{\left(\frac{\gamma_1(m,\rho_{sd})}{\gamma_2(m,\rho_{sr},\rho_{rd})}\right)^{mn-1}}{2\left(1-\frac{\gamma_1(m,\rho_{sd})}{\gamma_2(m,\rho_{sr},\rho_{rd})}\right)^{m(1+n)-1}} \left(\sum_{k=0}^{mn-1} \left(\frac{\gamma_2(m,\rho_{sr},\rho_{rd})}{\gamma_1(m,\rho_{sd})} - 1 \right)^k B_k I_k\left(\gamma_2(m,\rho_{sr},\rho_{rd})\right) \right.$$
$$\left. - \frac{\gamma_1(m,\rho_{sd})}{\gamma_2(m,\rho_{sr},\rho_{rd})} \sum_{k=0}^{m-1} \left(1-\frac{\gamma_1(m,\rho_{sd})}{\gamma_2(m,\rho_{sr},\rho_{rd})}\right)^k C_k I_k\left(\gamma_1(m,\rho_{sd})\right) \right)$$

where

$$A_k = (-1)^{mn-1+k} \frac{\binom{mn-1}{k}}{(mn-1)!} \prod_{\substack{n=1 \\ n\neq k+1}}^{mn} (m(1+n)-n), \qquad B_k = \frac{A_k}{\binom{m(1+n)-1}{k}}$$

$$C_k = \sum_{n=0}^{mn-1} \frac{\binom{k}{n}}{\binom{m(1+n)-1}{n}} A_n, \qquad I_k(c) = 1 - \sqrt{\frac{c}{1+c}} \left(1 + \sum_{n=1}^{k} \frac{(2n-1)!!}{n!2^n(1+c)^n}\right) \tag{37}$$

Authorized licensed use limited to: UNIVERSITY OF ALBERTA. Downloaded on January 20, 2010 at 12:24 from IEEE Xplore. Restrictions apply.

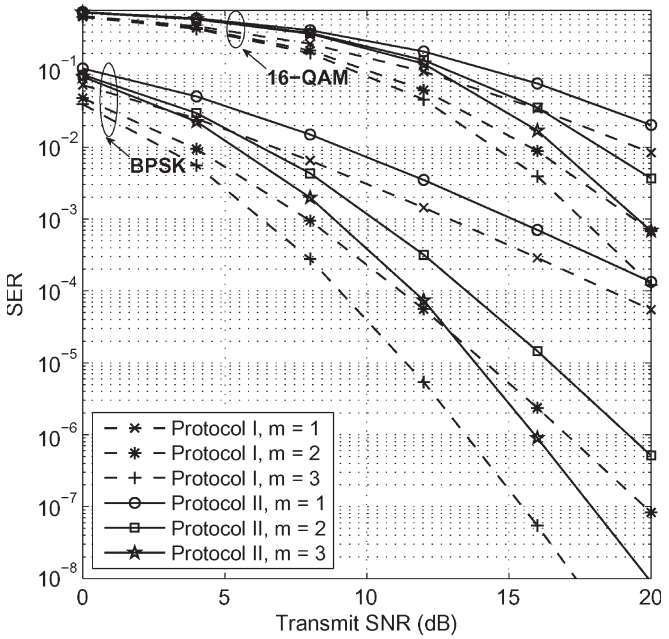

Fig. 6. SER comparison of Protocols I and II with BPSK and 16-QAM.

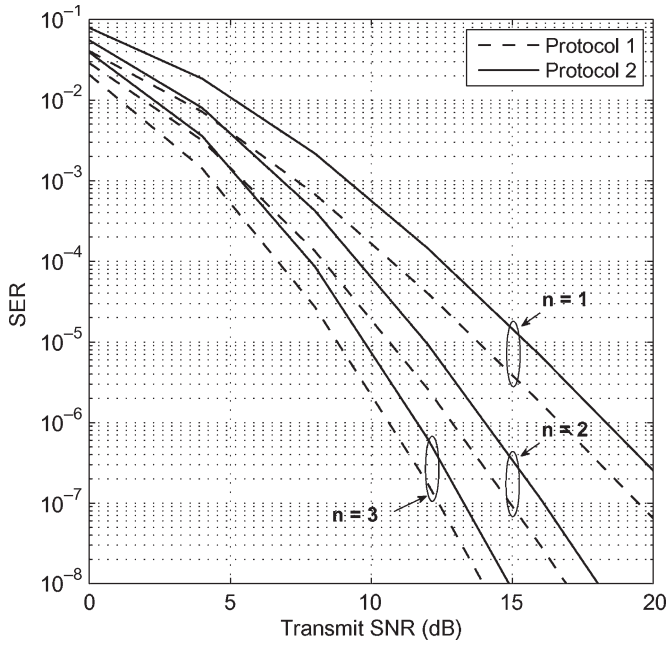

Fig. 7. SER variation for different number of cooperative nodes ($n = 1, 2,$ and 3) in Protocol I over Nakagami-2 fading for BPSK.

$2\rho_{sd}/m$ for Case 1 and Case 2, respectively. Therefore, the gap between two curves increases as m increases. Further, both cases have the same diversity order $(m+1)n$ at the high SNR region, as shown in Section V-B.

Fig. 6 compares the error performances of Protocols I and II for BPSK and 16-QAM under Case 1. Since the signals transmitted in the first and third time slots accrue diversity advantages by using Protocol I while utilizing the direct link $S \to D$, whereas the direct link is not utilized by Protocol II in the same time slots, in the equivalent high-SNR-approximated equations of (22) and (25) [(24) and (27)], the ρ_{sd}/m term appears in the former but not in the latter ($2\rho_{sd}/m$ term appears in the former while ρ_{sd}/m appears in the latter). Therefore, Protocol I performs better than Protocol II. The gap between the two protocols over medium and high SNR regions is almost constant, and they achieve same diversity order $(m+1)n$. The same analytical explanation as Fig. 5 holds here.

Fig. 7 shows the SER performance at a different number of cooperative nodes ($n = 1, 2,$ and 3) in a Nakagami-2 fading environment. As expected, the number of cooperative paths has a major impact on the performance of the network. A significant diversity order can be achieved by increasing the number of cooperative nodes because of the diversity advantage from the additional relay paths. For different n, the gap between two protocols is almost same in the high-SNR region because the MGFs of Protocols I and II have terms $[(2\rho_{sd}/m)(\rho_{sr}/m)^n]^m$ and $[(\rho_{sd}/m)(\rho_{sr}/m)^n]^m$ that change in the same order with n. Further, irrespective of the protocol, the diversity order is always $(n+1)m$, as in (33). Table II summarizes the end-to-end SNR and the significant term of the approximated high-SNR MGF of each protocol for different cases.

VII. Conclusion

We have analyzed the performance of two different TDMA-based cooperative protocols that are suitable for wireless/ad hoc networks. Our performance analysis is based on the versatile Nakagami-m distribution, which models a wide class of multipath fading channels. Closed-form MGFs of the total end-to-end SNR of a single-relay network with nonorthogonal channels, a single-relay network with orthogonal relay channels, and multiple-relay networks were derived. We showed that Protocol I has better capacity and SER performance. Orthogonal relaying, which ensures collision-free reception, has a lower SER because the destination receives independent relayed signals and direct-path signal. We also analyzed the two protocols in a multiple-relay scenario. The SER analysis reveals the diversity advantage. For instance, a diversity order of $(n+1)m$ is obtained for n parallel relays over Nakagami-m fading channels. SER expressions for $R_i \to D$ links with high SNRs and static $R_i \to D$ links are derived in closed form. The numerical and simulation results verify our analysis. Although only i.i.d. fading has been treated, our approach can be extended to independent and nonidentical Nakagami-m fading scenarios.

Appendix
Moment-Generating Function of End-to-End Signal-to-Noise Ratio

Case 1: To obtain the unconditional MGF, (21) should be averaged over all channel realizations. We assume that α_{sd}, α_{sr}, and α_{rd} are independent random variables. When α_{rd} is given, (21) can be written as

$$M_{\gamma\,|\,\alpha_{rd}}(t) = \mathbb{E}_{\alpha_{sr}}\left[\exp\left(-\frac{\left(\frac{\rho_{sr}\rho_{rd}}{\rho_{sr}+1}\right)\alpha_{sr}\alpha_{rd}}{\left(\frac{\rho_{rd}}{\rho_{sr}+1}\right)\alpha_{rd}+1}t\right)\right]$$

$$\times\,\mathbb{E}_{\alpha_{sd}}\left[\exp\left(-\frac{\rho_{sd}\left(\left(\frac{\rho_{rd}}{\rho_{sr}+1}\right)\alpha_{rd}+2\right)\alpha_{sd}}{\left(\frac{\rho_{rd}}{\rho_{sr}+1}\right)\alpha_{rd}+1}t\right)\right]. \quad (38)$$

Authorized licensed use limited to: UNIVERSITY OF ALBERTA. Downloaded on January 20, 2010 at 12:24 from IEEE Xplore. Restrictions apply.

TABLE II
SUMMERY OF SNR AND SIGNIFICANT TERM OF HIGH SNR MGF FOR EACH PROTOCOL

	Protocol I		Protocol II	
	SNR	MGF	SNR	MGF
Case 1	$\frac{[\lvert A\rvert^2+\lvert B\rvert^2+\lvert C\rvert^2]}{N_0}$	$\frac{1}{[(1+\frac{\rho_{sd}}{m}t)(1+\frac{\rho_{sr}}{m}t)]^m}$	$\frac{[\lvert B\rvert^2+\lvert C\rvert^2]}{N_0}$	$\frac{1}{[1+\frac{\rho_{sr}}{m}t]^m}$
Case 2	$\frac{[2\lvert A\rvert^2+\lvert B\rvert^2]}{N_0}$	$\frac{1}{\left[(1+\frac{2\rho_{sd}}{m}t)(1+\frac{\rho_{sr}}{m}t\right)]^m}$	$\frac{[\lvert A\rvert^2+\lvert B\rvert^2]}{N_0}$	$\frac{1}{[(1+\frac{\rho_{sd}}{m}t)(1+\frac{\rho_{sr}}{m}t)]^m}$
Case 3	$\frac{\left[2\lvert A\rvert^2+\sum_{i=1}^{n}\lvert B_i\rvert^2\right]}{N_0}$	$\frac{1}{\left[(1+\frac{2\rho_{sd}}{m}t)(1+\frac{\rho_{sr}}{m}t\right)^n]^m}$	$\frac{\left[\lvert A\rvert^2+\sum_{i=1}^{n}\lvert B_i\rvert^2\right]}{N_0}$	$\frac{1}{[(1+\frac{\rho_{sd}}{m}t)(1+\frac{\rho_{sr}}{m}t)^n]^m}$

Since α_{sr} and α_{sd} are gamma-distributed random variables, as given in (2), (38) can be averaged with respect to α_{sr} and α_{sd} to yield

$$M_{\gamma\,|\,\alpha_{rd}}(t)=\frac{1}{\left[\frac{\left(\frac{\rho_{sr}\rho_{rd}}{\rho_{sr}+1}\right)\alpha_{sr}\alpha_{rd}}{m\left(\frac{\rho_{rd}}{\rho_{sr}+1}\right)\alpha_{rd}+1}t+1\right]^m}\times\frac{1}{\left[\frac{\rho_{sd}\left(\left(\frac{\rho_{rd}}{\rho_{sr}+1}\right)\alpha_{rd}+2\right)\alpha_{sd}}{m\left(\frac{\rho_{rd}}{\rho_{sr}+1}\right)\alpha_{rd}+1}t+1\right]^m}. \quad (39)$$

After some algebraic manipulations, (39) can be written as

$$M_{\gamma\,|\,\alpha_{rd}}(t)=\frac{1}{\left[\left(1+\frac{\rho_{sr}}{m}t\right)\left(1+\frac{\rho_{sd}}{m}t\right)\right]^m}\times\frac{\left[\alpha_{rd}+\frac{\rho_{sr}+1}{\rho_{rd}}\right]^{2m}}{\left[\alpha_{rd}+\frac{\frac{\rho_{sr}+1}{\rho_{rd}}}{1+\frac{\rho_{sr}}{m}t}\right]^m\left[\alpha_{rd}+\frac{\left(\frac{\rho_{sr}+1}{\rho_{rd}}\right)\left(1+\frac{2\rho_{sd}}{m}t\right)}{1+\frac{\rho_{sd}}{m}t}\right]^m}. \quad (40)$$

Equation (40) can be rewritten in the form

$$M_{\gamma\,|\,\alpha_{rd}}(t)=\frac{[1+G(\alpha_{rd})]}{\left[\left(1+\frac{\rho_{sr}}{m}t\right)\left(1+\frac{\rho_{sd}}{m}\right)\right]^m} \quad (41)$$

where

$$G(\alpha_{rd})=\left[\frac{a_{2m-1}\alpha_{rd}^{2m-1}+\cdots+a_1\alpha_{rd}+a_0}{(\alpha_{rd}+\lambda_1(t))^m(\alpha_{rd}+\lambda_2(t))^m}\right]$$

with

$$\lambda_1(t)=\frac{\frac{\rho_{sr}+1}{\rho_{rd}}}{1+\frac{\rho_{sr}}{m}t},\quad \lambda_2(t)=\frac{\left(\frac{\rho_{sr}+1}{\rho_{rd}}\right)\left(1+\frac{2\rho_{sd}}{m}t\right)}{1+\frac{\rho_{sd}}{m}t}$$

and $a_{2m-1},\ldots,a_1,a_0$ as real constant coefficients of the numerator polynomial of the remainder, which can be evaluated by

$$\frac{\left(\alpha_{rd}+\frac{\rho_{sr}+1}{\rho_{rd}}\right)^{2m}}{[(\alpha_{rd}+\lambda_1(t))(\alpha_{rd}+\lambda_2(t))]^m}.$$

The right side of (41) can be decomposed into the partial fractions as

$$M_{\gamma\,|\,\alpha_{rd}}(t)=\frac{1}{\left[\left(1+\frac{\rho_{sr}}{m}t\right)\left(1+\frac{\rho_{sd}}{m}t\right)\right]^m}\times\left[1+\sum_{u=1}^{2}\sum_{v=1}^{m}\frac{A_{uv}(t)}{(\alpha_{rd}+\lambda_u(t))^v}\right] \quad (42)$$

where

$$A_{uv}(t)=\frac{1}{(m-v)!}\frac{d^{m-v}}{d\alpha_{rd}^{m-v}}\left[(\alpha_{rd}+\lambda_u(t))^m G(\alpha_{rd})\right]$$

is evaluated at $\alpha_{rd}=-\lambda_u(t)$. Since the fading effects of the link between relay R and destination D are modeled as Nakagami-m fading, the unconditional MGF is derived by averaging (42) over α_{rd} to yield

$$M_{\gamma}(t)=\frac{1}{\left[\left(1+\frac{\rho_{sr}}{m}t\right)\left(1+\frac{\rho_{sd}}{m}t\right)\right]^m}\times\left[1+\sum_{u=1}^{2}\sum_{v=1}^{m}m^m A_{uv}(t)\left[\lambda_u(t)\right]^{m-v}\times\psi\left(m,m-v+1,m\lambda_u(t)\right)\right] \quad (43)$$

where $\psi(\alpha;\beta;z)$ is the confluent hypergeometric function of the second kind [31, eq. (9.211.4)]. This completes the closed-form MGF derivation for Protocol I with Case 1.

Case 2 and Case 3: Let us consider the notations $\lvert h_{sr_i}\rvert^2=\alpha_{sr_i}$ and $\lvert h_{r_id}\rvert^2=\alpha_{r_id}$ for the sake of convenience. Then, (23) can further be written as

$$\gamma=\left[2\rho_{sd}\alpha_{sd}+\sum_{i=1}^{n}\frac{\frac{\rho_{sr}\rho_{rd}}{\rho_{sr}+1}}{\left(\frac{\rho_{rd}}{\rho_{sr}+1}\alpha_{r_id}+1\right)}\alpha_{sr_i}\alpha_{r_id}\right]. \quad (44)$$

Assuming that α_{sd}, α_{sr_i}, and α_{r_id} are mutually independent random variables, $\forall i=1,2,\ldots,n$. When all α_{r_id}'s are given, the conditional MGF can be written as

$$M_{\gamma\,|\,\alpha_{r_id}}(t)=\mathbb{E}_{\alpha_{sd}}\left[\exp(-2\rho_{sd}\alpha_{sd}t)\right]\times\prod_{i=1}^{n}\mathbb{E}_{\alpha_{sr_i}}\left[\exp\left(-\frac{\frac{\rho_{sr}\rho_{rd}}{\rho_{sr}+1}\alpha_{sr_i}\alpha_{r_id}}{\left(\frac{\rho_{rd}}{\rho_{sr}+1}\alpha_{r_id}+1\right)}t\right)\right]. \quad (45)$$

Since α_{sr_i} and α_{sd} are gamma-distributed random variables, as given in (2), (45) can be averaged with respect to α_{sr_i} and α_{sd} to yield

$$M_{\gamma\,|\,\alpha_{r_id}}(t)=\frac{1}{\left[1+\frac{2\rho_{sd}}{m}t\right]^m}\prod_{i=1}^{n}\frac{1}{\left[1+\frac{\left(\frac{\rho_{sr}\rho_{rd}}{\rho_{sr}+1}\right)\alpha_{r_id}}{m\left(\frac{\rho_{rd}}{\rho_{sr}+1}\alpha_{r_id}+1\right)}t\right]^m}. \quad (46)$$

Authorized licensed use limited to: UNIVERSITY OF ALBERTA. Downloaded on January 20, 2010 at 12:24 from IEEE Xplore. Restrictions apply.

After some simple algebraic manipulations, (46) can be written as

$$M_{\gamma\,|\,\alpha_{r_i d}}(t) = \frac{1}{\left[\left(1+\frac{2\rho_{sd}}{m}t\right)\left(1+\frac{\rho_{sr}}{m}t\right)^n\right]^m}\prod_{i=1}^{n}\left[1+H(\alpha_{r_i d})\right] \tag{47}$$

where

$$H(\alpha_{r_i d}) = \frac{\left(b_{m-1}\alpha_{r_i d}^{m-1}+\cdots+b_1\alpha_{r_i d}+b_0\right)}{\left(\alpha_{r_i d}+\mu(t)\right)^m}$$

with $\mu(t) = ((\rho_{sr}+1)/\rho_{rd})/(1+(\rho_{sr}/m)t)$, and similar to the previous case, $b_{m-1},\ldots,b_1,b_0$ are real constant coefficients of the numerator of the remainder polynomial. The right side of (47) can be decomposed into partial fractions as

$$M_{\gamma\,|\,\alpha_{r_i d}}(t) = \frac{1}{\left[\left(1+\frac{2\rho_{sd}}{m}t\right)\left(1+\frac{\rho_{sr}}{m}t\right)^n\right]^m} \times\prod_{i=1}^{n}\left[1+\sum_{v=1}^{m}\frac{A_v(t)}{\left(\alpha_{r_i d}+\mu(t)\right)^v}\right] \tag{48}$$

where

$$A_v(t) = \frac{1}{(m-v)!}\frac{d^{m-v}}{d\alpha_{r_i d}^{m-v}}\left[(\alpha_{r_i d}+\mu(t))^m H(\alpha_{r_i d})\right]\Big|_{\alpha_{r_i d}=-\mu(t)}.$$

Therefore, the closed-form solution for the unconditional MGF of γ can be expressed as

$$M_\gamma(t) = \frac{1}{\left[\left(1+\frac{2\rho_{sd}}{m}t\right)\left(1+\frac{\rho_{sr}}{m}t\right)^n\right]^m} \times\left[1+\sum_{v=1}^{m}A_v(t)m^m\left[\mu(t)\right]^{m-v} \times\psi\left(m,m+1-v,m\mu(t)\right)\right]^n. \tag{49}$$

REFERENCES

[1] A. Sendonaris, E. Erkip, and B. Aazhang, "User cooperation diversity. Part I: System description," *IEEE Trans. Commun.*, vol. 51, no. 11, pp. 1927–1938, Nov. 2003.

[2] A. Sendonaris, E. Erkip, and B. Aazhang, "User cooperation diversity. Part II. Implementation aspects and performance analysis," *IEEE Trans. Commun.*, vol. 51, no. 11, pp. 1939–1948, Nov. 2003.

[3] J. N. Laneman, D. N. C. Tse, and G. W. Wornell, "Cooperative diversity in wireless networks: Efficient protocols and outage behavior," *IEEE Trans. Inf. Theory*, vol. 50, no. 12, pp. 3062–3080, Dec. 2004.

[4] V. Genc, S. Murphy, Y. Yu, and J. Murphy, "IEEE 802.16j relay-based wireless access networks: An overview," *Wireless Commun.*, vol. 15, no. 5, pp. 56–63, Oct. 2008, [recent advances and evolution of WLAN and WMAN standards].

[5] C. Patel, G. Stuber, and T. Pratt, "Statistical properties of amplify and forward relay fading channels," *IEEE Trans. Veh. Technol.*, vol. 55, no. 1, pp. 1–9, Jan. 2006.

[6] A. Kwasinski and K. Liu, "Source-channel-cooperation tradeoffs for adaptive coded communications," *IEEE Trans. Wireless Commun.*, vol. 7, no. 9, pp. 3347–3358, Sep. 2008.

[7] J. W. Mark and W. Zhuang, *Wireless Communications and Networking*. Upper Saddle River, NJ: Prentice-Hall, 2003.

[8] H. Jiang and W. Zhuang, "Quality-of-service provisioning in future 4G CDMA cellular networks," *IEEE Wireless Commun.*, vol. 11, no. 2, pp. 48–54, Apr. 2004.

[9] H. Jiang, W. Zhuang, X. Shen, and Q. Bi, "Quality-of-service provisioning and efficient resource utilization in CDMA cellular communications," *IEEE J. Sel. Areas Commun.*, vol. 24, no. 1, pp. 4–15, Jan. 2006.

[10] R. U. Nabar, H. Bolcskei, and F. W. Kneubuhler, "Fading relay channels: Performance limits and space–time signal design," *IEEE J. Sel. Areas Commun.*, vol. 22, no. 6, pp. 1099–1109, Aug. 2004.

[11] J. Laneman and G. Wornell, "Distributed space–time-coded protocols for exploiting cooperative diversity in wireless networks," *IEEE Trans. Inf. Theory*, vol. 49, no. 10, pp. 2415–2425, Oct. 2003.

[12] Y. Jing and B. Hassibi, "Distributed space–time coding in wireless relay networks," *IEEE Trans. Wireless Commun.*, vol. 5, no. 12, pp. 3524–3536, Dec. 2006.

[13] T. A. Tsiftsis, G. K. Karagiannidis, S. A. Kotsopoulos, and F. N. Pavlidou, "BER analysis of collaborative dual-hop wireless transmissions," *Electron. Lett.*, vol. 40, no. 11, pp. 679–681, May 2004.

[14] A. Ribeiro, X. Cai, and G. B. Giannakis, "Symbol error probabilities for general cooperative links," *IEEE Trans. Wireless Commun.*, vol. 4, no. 3, pp. 1264–1273, May 2005.

[15] S. Ikki and M. H. Ahmed, "Performance analysis of cooperative diversity wireless networks over Nakagami-m fading channel," *IEEE Commun. Lett.*, vol. 11, no. 4, pp. 334–336, Apr. 2007.

[16] Y. Li and S. Kishore, "Asymptotic analysis of amplify-and-forward relaying in Nakagami-fading environments," *IEEE Trans. Wireless Commun.*, vol. 6, no. 12, pp. 4256–4262, Dec. 2007.

[17] S. S. Ikki and M. H. Ahmed, "Performance of multiple-relay cooperative diversity systems with best relay selection over Rayleigh fading channels," *EURASIP J. Adv. Signal Process.*, vol. 8, no. 2, pp. 1–7, Jan. 2008.

[18] M. Hasna and M.-S. Alouini, "Harmonic mean and end-to-end performance of transmission systems with relays," *IEEE Trans. Commun.*, vol. 52, no. 1, pp. 130–135, Jan. 2004.

[19] G. K. Karagiannidis, T. A. Tsiftsis, and R. K. Mallik, "Bounds for multihop relayed communications in Nakagami-m fading," *IEEE Trans. Commun.*, vol. 54, no. 1, pp. 18–22, Jan. 2006.

[20] S. Atapattu and N. Rajatheva, "Exact SER of Alamouti code transmission through amplify-forward cooperative relay over Nakagami-m fading channels," in *Proc. ISCIT*, Aug. 2007, pp. 1429–1433.

[21] S. Atapattu and N. Rajatheva, "Performance evaluation of Alamouti STC through amplify-forward cooperative relay network over Nakagami-m fading channels," in *Proc. FGCN*, Dec. 2007, vol. 2, pp. 258–263.

[22] S. Atapattu and N. Rajatheva, "Analysis of Alamouti code transmission over TDMA-based cooperative protocol," in *Proc. IEEE VTC*, May 2008, pp. 1226–1230.

[23] A. Annamalai and C. Tellambura, "Error rates for Nakagami-m fading multichannel reception of binary and M-ary signals," *IEEE Trans. Commun.*, vol. 49, no. 1, pp. 58–68, Jan. 2001.

[24] K. Azarian, H. El Gamal, and P. Schniter, "On the achievable diversity-multiplexing tradeoff in half-duplex cooperative channels," *IEEE Trans. Inf. Theory*, vol. 51, no. 12, pp. 4152–4172, Dec. 2005.

[25] Y. Song, M. Sarkar, and H. Shin, "Cooperative diversity with blind relays in Nakagami-m fading channels: MRC analysis," in *Proc. IEEE VTC*, May 2008, pp. 1196–1200.

[26] B. Maham and A. Hjorungnes, "Symbol error rate of amplify-and-forward distributed space–time codes over Nakagami-m fading channel," *Electron. Lett.*, vol. 45, no. 3, pp. 174–175, Jan. 2009.

[27] S. Alamouti, "A simple transmit diversity technique for wireless communications," *IEEE J. Sel. Areas Commun.*, vol. 16, no. 8, pp. 1451–1458, Oct. 1998.

[28] M. Nakagami, "The m-distribution as general formula for intensity distribution of rapid fading," in *Statistical Methods in Radio Wave Propagation*. Oxford, U.K.: Pergamon, 1960.

[29] M. K. Simon and M.-S. Alouini, *Digital Communication Over Fading Channels*, 2nd ed. New York: Wiley, 2005.

[30] C. Tellambura, A. J. Mueller, and V. K. Bhargava, "Analysis of M-ary phase-shift keying with diversity reception for land–mobile satellite channels," *IEEE Trans. Veh. Technol.*, vol. 46, no. 4, pp. 910–922, Nov. 1997.

[31] I. S. Gradshteyn and I. M. Ryzhik, *Table of Integrals, Series, and Products*, 6th ed. New York: Academic, 2000.

[32] Z. Wang and G. B. Giannakis, "A simple and general parameterization quantifying performance in fading channels," *IEEE Trans. Commun.*, vol. 51, no. 8, pp. 1389–1398, Aug. 2003.

[33] L. C. Andrews, *Special Functions of Mathematics for Engineers*, 2nd ed. Hoboken, NJ: SPIE, 1998.

Authorized licensed use limited to: UNIVERSITY OF ALBERTA. Downloaded on January 20, 2010 at 12:24 from IEEE Xplore. Restrictions apply.

Saman Atapattu (S'06) received the B.Sc. degree in electrical and electronics engineering (with first-class honors) from the University of Peradeniya, Peradeniya, Sri Lanka, in 2003 and the M.Eng. degree in telecommunications from the Asian Institute of Technology, Pathumthani, Thailand, in 2007. He is currently working toward the Ph.D. degree in electrical engineering with the University of Alberta, Edmonton, AB, Canada.

His research interests include cooperative communications, spectrum sensing in cognitive radio, energy detection, and performance analysis of communication systems.

Nandana Rajatheva (SM'01) received the B.Sc. degree in electronics and telecommunication engineering (with first-class honors) from the University of Moratuwa, Moratuwa, Sri Lanka, in 1987 and the M.Sc. and the Ph.D. degrees from the University of Manitoba, Winnipeg, MB, Canada, in 1991 and 1995, respectively.

From May 1996 to December 2001, he was an Associate Professor with Telecommunications—School of Advanced Technology. He was also with the University of Moratuwa, where he became a Professor of electronics and telecommunication engineering in June 2003. He is currently an Associate Professor of telecommunications with the School of Engineering and Technology, Asian Institute of Technology, Pathumthani, Thailand. He is an Editor for the *International Journal of Vehicular Technology* (Hindawi). His research interests include digital and mobile communications, cooperative diversity, relay systems, orthogonal frequency-division multiple access resource allocation, detection/estimation techniques in cognitive radio, space–time processing multiple-input–multiple-output systems, and distributed video coding.

Dr. Rajatheva is a Senior Member of the IEEE Communications and Vehicular Technology Societies.

Chintha Tellambura (SM'02) received the B.Sc. degree (with first-class honors) from the University of Moratuwa, Moratuwa, Sri Lanka, in 1986, the M.Sc. degree in electronics from the University of London, London, U.K., in 1988, and the Ph.D. degree in electrical engineering from the University of Victoria, Victoria, BC, Canada, in 1993.

He was a Postdoctoral Research Fellow with the University of Victoria from 1993 to 1994 and with the University of Bradford, Bradford, U.K., from 1995 to 1996. From 1997 to 2002, he was with Monash University, Clayton, Australia. He is currently a Professor with the Department of Electrical and Computer Engineering, University of Alberta, Edmonton, AB, Canada. His research interests include diversity and fading countermeasures, multiple-input–multiple-output systems, space–time coding, and orthogonal frequency-division multiplexing.

Prof. Tellambura is an Associate Editor for the IEEE TRANSACTIONS ON COMMUNICATIONS and the Area Editor for Wireless Communications Systems and Theory for the IEEE TRANSACTIONS ON WIRELESS COMMUNICATIONS. He was the Chair of the Communication Theory Symposium at Globecom'05 held in St. Louis, MO.

Authorized licensed use limited to: UNIVERSITY OF ALBERTA. Downloaded on January 20, 2010 at 12:24 from IEEE Xplore. Restrictions apply.